

Syntheses, Characterization, Redox Properties, and Mixed-Valence Chemistry of Tetra- and Hexanuclear Diyndiyl Complexes

Li-Bin Gao,[†] Li-Yi Zhang,[†] Lin-Xi Shi,[†] and Zhong-Ning Chen^{*,†,‡}

State Key Laboratory of Structural Chemistry, Fujian Institute of Research on the Structure of Matter and Graduate School of CAS, Chinese Academy of Sciences, Fuzhou, Fujian 350002, China, and State Key Laboratory of Organometallic Chemistry, Shanghai Institute of Organic Chemistry, Chinese Academy of Sciences, Shanghai 200032, China

Received November 24, 2004

A series of Ru^{II}₂Fe^{II}₂ heterotetranuclear σ -acetylide complexes [$\{\text{Cp}(\text{dppf})\text{Ru}\}_2(\text{C}\equiv\text{C}-\text{R}-\text{C}\equiv\text{C})$] (dppf = 1,1'-bis(diphenylphosphino)ferrocene, R = 0, **1**; 1,4-benzenediyl, **2**; 1,4-naphthalenediyl, **3**; 9,10-anthracenediyl, **4**) were prepared and characterized by elemental analyses, ES-MS spectrometry, IR, ¹H and ³¹P NMR, and UV-vis-NIR spectroscopy, and cyclic and differential pulse voltammetry. Reaction of **1** with [Cu(MeCN)₄](ClO₄) gave Ru^{II}₂-Fe^{II}₂Cu^I heterohexanuclear compound [$\{\text{Cp}(\text{dppf})\text{Ru}\}_2\{\text{Cu}(\text{MeCN})_2(\text{C}\equiv\text{C}-\text{C}\equiv\text{C})\}(\text{ClO}_4)_2$] [**5**(ClO₄)₂] through π -bonding of the acetylides to Cu^I centers. The structures of **1** and **5**(ClO₄)₂ (SbF₆) were determined by X-ray crystallography. Chemical oxidation of **1**, **3**, and **4** with an equivalent of ferrocenium hexafluorophosphate gave one-electron-oxidized species [$\{\text{Cp}(\text{dppf})\text{Ru}\}_2(\text{C}\equiv\text{C}-\text{R}-\text{C}\equiv\text{C})$](PF₆) [R = 0, **1a**(PF₆); 1,4-naphthalenediyl, **3a**(PF₆); 9,10-anthracenediyl, **4a**(PF₆)] with Ru^{II,III} mixed valence. Electrochemical and visible-infrared spectral studies revealed that the electronic delocalization depends on the R substituent in the bridging ligand C≡C-R-C≡C. While the mixed-valence compound **1a**(PF₆) (R = 0) displays an electronically delocalized behavior (class III mixed-valence system), **3a**(PF₆) (R = 1,4-naphthalenediyl) and **4a**(PF₆) (R = 9,10-anthracenediyl) may belong to borderline compounds between electronic localization and delocalization.

Introduction

Metal complexes with a conjugated carbon bridge have currently attracted great attention because of their potential applications in molecular electronics.^{1–8} The rodlike metal polyacetylide complexes L_mM-(C≡C)_n-

ML_m (n = 1, 2, 3, L) are of particular efficiency in transmitting electronic interaction between two redox-active metal termini through a conjugated rigid -(C≡C)_n- ligand.^{9–11} Many diyndiyl compounds L_mM-C≡C-C≡C-ML_m containing various redox-active metal centers have been prepared, some of which have been characterized by X-ray crystallography.^{10–17} These redox-active metal termini include Cp*(dppe)Fe,¹¹ X-(dmpm)₂Mn (X = I, C≡CH),¹² Cp*(CO)₂Fe*,¹³ Cp(PPh₃)₂-

* To whom correspondence should be addressed. E-mail: czn@ms.fjirsm.ac.cn.

[†] State Key Laboratory of Structural Chemistry.

[‡] State Key Laboratory of Organometallic Chemistry.

(1) General reviews or accounts: (a) Paul, F.; Lapinte, C. *Coord. Chem. Rev.* **1998**, *178–180*, 431–509. (b) Szafer, S.; Gladysz, J. A. *Chem. Rev.* **2003**, *103*, 4175–4206. (c) Long, N. J.; Williams, C. K. *Angew. Chem., Int. Ed.* **2003**, *42*, 2586–2617. (d) Ziesse, R.; Hissler, M.; El-ghayoury, A.; Harriman, A. *Coord. Chem. Rev.* **1998**, *178–180*, 1251–1298. (e) Touchard, D.; Dixneuf, P. H. *Coord. Chem. Rev.* **1998**, *178–180*, 409–429. (f) Martin, R. E.; Diederich, F. *Angew. Chem., Int. Ed.* **1999**, *38*, 1350–1377. (g) Hurst, T. K.; Ren, T. *J. Organomet. Chem.* **2003**, *670*, 188–197. (h) Akita, M.; Sakurai, A.; Chung, M.-C.; Morooka, Y. *J. Organomet. Chem.* **2003**, *670*, 2–10.

(2) (a) Chung, M. C.; Gu, X.; Etzenhouser, B. A.; Spuches, A. M.; Rye, P. T.; Seetharaman, S. K.; Rose, D. J.; Zubieta, J.; Sponsler, M. B. *Organometallics* **2003**, *22*, 3485–3494. (b) Etzenhouser, B. A.; Cavanaugh, M. D.; Spurgeon, H. N.; Sponsler, M. B. *J. Am. Chem. Soc.* **1994**, *116*, 2221–2222. (c) Etzenhouser, B. A.; Chen, Q.; Sponsler, M. B. *Organometallics* **1994**, *13*, 4176–4178.

(3) (a) Liu, S. H.; Chen, Y.; Wan, K. L.; Wen, T. B.; Zhou, Z.; Lo, M. F.; Williams, I. D.; Jia, G. *Organometallics* **2002**, *21*, 4984–4992. (b) Liu, S. H.; Xia, H.; Wen, T. B.; Zhou, Z. Y.; Jia, G. *Organometallics* **2003**, *22*, 737–743. (c) Xia, H. P.; Ng, W. S.; Ye, J. S.; Li, X. Y.; Wong, W. T.; Lin, Z.; Yang, C.; Jia, G. *Organometallics* **1999**, *18*, 4552–4557. (d) Xia, H. P.; Wu, W. F.; Ng, W. S.; Williams, I. D.; Jia, G. *Organometallics* **1997**, *16*, 2940–2947.

(4) Adams, R. D.; Qu, B.; Smith, M. D. *Inorg. Chem.* **2001**, *40*, 2932–2934.

(5) (a) Zhu, Y.; Clot, O.; Wolf, M. O.; Yap, G. P. A. *J. Am. Chem. Soc.* **1998**, *120*, 1812–1821. (b) Iyer, R. S.; Selegue, J. P. *J. Am. Chem. Soc.* **1987**, *109*, 910–911.

(6) (a) Shi, Y.; Yee, G. T.; Wang, G.; Ren, T. *J. Am. Chem. Soc.* **2004**, *126*, 10552–10553. (b) Xu, G.-L. DeRosa, M. C.; Crutchley, R. J.; Ren, T. *J. Am. Chem. Soc.* **2004**, *126*, 3728–3729. (c) Wong, K.-T.; Lehn, J.-M.; Peng, S.-M.; Lee, G.-H. *Chem. Commun.* **2000**, 2259–2260.

(7) (a) Uno, M.; Dixneuf, P. H. *Angew. Chem., Int. Ed.* **1998**, *37*, 1714–1717. (b) Rigaut, S.; Perruchon, J.; Pichon, L. L.; Touchard, D.; Dixneuf, P. H. *J. Organomet. Chem.* **2003**, *670*, 37–44. (c) Rigaut, S.; Pichon, L. L.; Daran, J.-C.; Touchard, D.; Dixneuf, P. H. *Chem. Commun.* **2001**, 1206–1207. (d) Rigaut, S.; Touchard, D.; Dixneuf, P. H. *J. Organomet. Chem.* **2003**, *684*, 68–76.

(8) Field, L. D.; Turnbull, A. J.; Turner, P. *J. Am. Chem. Soc.* **2002**, *124*, 3692–3702.

(9) (a) Antonova, A.; Bruce, M. I.; Ellis, B. G.; Gaudio, M.; Humphrey, P. A.; Jevric, M.; Melino, G.; Nicholson, B. K.; Perkins, G. J.; Skelton, B. W.; Stapleton, B.; White, A. H.; Zaitseva, N. N. *Chem. Commun.* **2004**, 960–961. (b) Bruce, M. I.; Ellis, B. G.; Gaudio, M.; Lapinte, C.; Melino, G.; Paul, F.; Skelton, B. W.; Smith, M. E.; Toupet, L.; White, A. H. *J. Chem. Soc., Dalton Trans.* **2004**, 1601–1609.

(10) (a) Dembinski, R.; Bartik, T.; Bartik, B.; Jaeger, M.; Gladysz, J. A. *J. Am. Chem. Soc.* **2000**, *122*, 810–822. (b) Brady, M.; Weng, W.; Zhou, Y.; Seyler, J. W.; Amoroso, A. J.; Arif, A. M.; Böhme, M.; Frenking, G.; Gladysz, J. A. *J. Am. Chem. Soc.* **1997**, *119*, 775–788. (c) Jiao, H.; Costuas, K.; Gladysz, J. A.; Halet, J.-F.; Guillemot, M.; Toupet, L.; Paul, F.; Lapinte, C. *J. Am. Chem. Soc.* **2003**, *125*, 9511–9522. (d) Horn, C. R.; Gladysz, J. A. *J. Eur. Inorg. Chem.* **2003**, 2211–2218. (e) Horn, C. R.; Martin-Alvarez, J. M.; Gladysz, J. A. *Organometallics* **2002**, *21*, 5386–5393.

Ru,¹⁴ Cp*(dppe)Ru,¹⁵ Cp*(NO)(PR₃)Re (R = aryl),¹⁰ Cl(PPr₃)₂HRh/Ir,¹⁶ and Ru₂(ap)₄,¹⁷ etc. It has been demonstrated that remarkable electronic communication is mediated through the C₄ chains with redox wave separation between two organometallic redox centers in the range 0.50–0.80 V, and consequently, the comproportionation constant *K*_c can be as high as 10¹³.^{10–17}

Comparing with numerous C₄-bridged compounds, diacetylide C≡C–R–C≡C (R = aryl)-linked metal complexes L_mM–C≡C–R–C≡C–ML_m are much fewer.^{18–21} It has been revealed that a moderate electronic delocalization occurs in the dinuclear compounds L_mM–C≡C–C₆H₄–C≡C–ML_m with potential difference between two metal centers in the range 0.20–0.30 V.^{20,21} Recently, diacetylide C≡C–R–C≡C-linked dinuclear platinum(II) complexes have also been prepared and characterized by X-ray crystallography when R = 1,4-naphthalenediyl or 1,10-anthracenediyl.¹⁸ To the best of our knowledge, dinuclear complexes with redox-active ruthenium termini bridged by C≡C–R–C≡C with R = 1,4-naphthalenediyl or 1,10-anthracenediyl, however, have not yet been reported.

In contrast with one redox center in most of the redox-active metal termini, Cp(dppf)RuCl, containing a redox-active peripheral ligand dppf, can afford two redox centers. Stepwise oxidation of Ru^{II} and Fe^{II} centers in Cp(dppf)RuCl induces two reversible one-electron waves. It is expected that diacetylide-linked complexes Cp(dppf)Ru–C≡C–R–C≡C–Ru(dppf)Cp containing both

Ru and Fe as redox centers would exhibit richer electronic interactions and multiple redox properties because electronic communication would occur in Ru and Fe redox centers, respectively. Furthermore, the electronic effect mediated by the bridging ligand C≡C–R–C≡C is likely tunable by modification of the π-conjugating degree of the R substituent.

Aiming at addressing the issues mentioned above, a series of heterotetranuclear complexes [{Cp(dppf)Ru}₂(C≡C–R–C≡C)] (R = 0, **1**; 1,4-benzenediyl, **2**; 1,4-naphthalenediyl, **3**; 9,10-anthracenediyl, **4**) and their one-electron-oxidized species [{Cp(dppf)Ru}₂(C≡C–R–C≡C)](PF₆) [R = 0, **1a**(PF₆); 1,4-naphthalenediyl, **3a**(PF₆); 9,10-anthracenediyl, **4a**(PF₆)] with Ru₂^{II,III} mixed-valence were prepared and characterized by spectroscopic and electrochemical methods. Considering that in the heterotetranuclear compound [{Cp(dppf)Ru}₂(C≡C–C≡C)] (**1**) the σ-acetylides can further be bound to Cu^I ion through π-coordination, heterohexanuclear compound [{Cp(dppf)Ru}₂{Cu(MeCN)}₂(C≡C–C≡C)](ClO₄)₂ [5(ClO₄)₂] was prepared by reaction of **1** with [Cu(MeCN)₄](ClO₄) in order to detect the influence of acetylide π-bonding on the electronic communication between two redox termini Cp(dppf)Ru.

Experimental Section

General Material. The manipulations were carried out in an atmosphere of dry argon by using standard Schlenk techniques. The solvents were dried, distilled, and degassed before use except that those for UV–vis–NIR spectral measurements were of spectroscopic grade. The reagents ruthenium(III) chloride hydrate, 1,4-bis(trimethylsilyl)-1,3-butadiyne, potassium hexafluorophosphate, ferrocenium hexafluorophosphate, and 1,2-bis(diphenylphosphino)ferrocene (dppf) were commercially available (Acros or Strem Chemicals). The compounds Cp(dppf)RuCl²² and [Cu(MeCN)₄](ClO₄)²³ were synthesized by the literature methods. The diacetylene ligands 1,4-bis(trimethylsilylethynyl)naphthalene and 9,10-bis(trimethylsilylethynyl)anthracene were prepared by modified procedures described in the literature.¹⁸

[{Cp(dppf)Ru}₂(C≡C–C≡C)] (**1**). To 60 mL of methanol–tetrahydrofuran (5:1) were first added 1,4-bis(trimethylsilyl)-1,3-butadiyne (64.0 mg, 0.33 mmol) and potassium fluoride (40.0 mg, 0.66 mmol), then Cp(dppf)RuCl (500.0 mg, 0.66 mmol). After the solution was stirred under reflux for 1 day, the solvent was evaporated in vacuo. The product was purified by chromatography on a neutral alumina column using dichloromethane as an eluent to collect the orange band. Layering petroleum ether onto the dichloromethane solution afforded orange crystals. Yield: 62%. Anal. Calcd for C₈₂H₆₆Fe₂P₄Ru₂·3CH₂Cl₂: C, 58.54; H, 4.16. Found: C, 58.71; H, 4.03. ESI-MS: *m/z* (%) 1490 (100) [M]⁺, 721 (8) [Cp(dppf)Ru]⁺. IR (KBr, cm⁻¹): ν 1968m (C≡C). ¹H NMR (CDCl₃, ppm): δ 7.78–7.26 (m, 40H, C₆H₅), δ 5.29 (s, 6H, CH₂Cl₂), δ 5.18, 4.33, 4.23, 4.02 (four singlets, 16H, (C₅H₄)₂Fe) and 4.11(s, 10H, CpRu). ³¹P NMR (CD₂Cl₂): δ 55.7 (s). UV–vis (CH₂Cl₂): λ_{max}/nm (ε/M⁻¹ cm⁻¹) = 306 (24260), 364 (8490).

[{Cp(dppf)Ru}₂(C≡C–R–C≡C)] (R = 1,4-benzenediyl, **2**). To 60 mL of methanol were added Cp(dppf)RuCl (500.0 mg, 0.66 mmol) and potassium hexafluorophosphate (150.0 mg, 0.82 mmol). After the suspended solution was refluxed for 30 min, to which was added 1,4-diethynylbenzene (42.0 mg, 0.33 mmol). The orange solution continued to reflux for 15 min and then put aside to cool at room temperature. Addition of sodium methoxide (107.0 mg, 1.98 mmol) resulted in a yellow precipi-

(11) (a) Paul, F.; Meyer, W. E.; Toupet, L.; Jiao, H.; Gladysz, J. A.; Lapinte, C. *J. Am. Chem. Soc.* **2000**, *122*, 9405–9414. (b) Narvor, N. L.; Toupet, L.; Lapinte, C. *J. Am. Chem. Soc.* **1995**, *117*, 7129–7138. (c) Courmarcel, J.; Gland, G. L.; Toupet, L.; Paul, F.; Lapinte, C. *J. Organomet. Chem.* **2003**, *670*, 108–122. (d) Guillaume, V.; Mahias, V.; Mari, A.; Lapinte, C. *Organometallics* **2000**, *19*, 1422–1426. (e) Coat, F.; Guillevic, M.-A.; Toupet, L.; Paul, F.; Lapinte, C. *Organometallics* **1997**, *16*, 5988–5998.

(12) (a) Kheradmandan, S.; Heinze, K.; Schmalle, H. W.; Berke, H. *Angew. Chem., Int. Ed.* **1999**, *38*, 2270–2273. (b) Fernández, F. J.; Venkatesan, K.; Blaque, O.; Alfonso, M.; Schmalle, H. W.; Berke, H. *Chem. Eur. J.* **2003**, *9*, 6192–6206.

(13) Akita, M.; Chung, M.-C.; Sakurai, A.; Sugimoto, S.; Terada, M.; Tanaka, M.; Moro-oka, Y. *Organometallics* **1997**, *16*, 4882–4888.

(14) (a) Bruce, M. I.; Low, P. J.; Costuas, K.; Halet, J.-F.; Best, S. P.; Heath, G. A. *J. Am. Chem. Soc.* **2000**, *122*, 1949–1962. (b) Bruce, M. I.; Hall, B. C.; Kelly, B. D.; Low, P. J.; Skelton, B. W.; White, A. H. *J. Chem. Soc., Dalton Trans.* **1999**, 3719–3728. (c) Bruce, M. I.; Hinterding, P.; Tiekink, E. R. T.; Skelton, B. W.; White, A. H. *J. Organomet. Chem.* **1993**, *450*, 209–218.

(15) Bruce, M. I.; Ellis, B. G.; Low, P. J.; Skelton, B. W.; White, A. H. *Organometallics* **2003**, *22*, 3184–3198.

(16) (a) Gil-Rubio, J.; Laubender, M.; Werner, H. *Organometallics* **2000**, *19*, 1365–1372. (b) Gil-Rubio, J.; Laubender, M.; Werner, H. *Organometallics* **1998**, *17*, 1202–1207. (c) Gevert, O.; Wolf, J.; Werner, H. *Organometallics* **1996**, *15*, 2806–2809.

(17) (a) Ren, T.; Zou, G.; Alvarez, J. C. *Chem. Commun.* **2000**, 1197–1198. (b) Xu, G.-L.; Zou, G.; Ni, Y.-H.; DeRosa, M. C.; Crutchley, R. J.; Ren, T. *J. Am. Chem. Soc.* **2003**, *125*, 10057–10065.

(18) Khan, M. S.; Al-Mandhary, M. R. A.; Al-Suti, M. K.; Al-Battashi, F. R.; Al-Saadi, S.; Ahrens, B.; Bjernemose, J. K.; Mahon, M. F.; Raithby, P. R.; Younus, M.; Chawdhury, N.; Köhler, A.; Marseglia, E. A.; Tedesco, E.; Feeder, N.; Teat, S. J. *J. Chem. Soc., Dalton Trans.* **2004**, 2377–2385.

(19) (a) Colbert, M. C. B.; Lewis, J.; Long, N. J.; Raithby, P. R.; Younus, M.; White, A. J. P.; Williams, D. J.; Payne, N. N.; Yellowlees, L.; Beljonne, D.; Chawdhury, N.; Friend, R. H. *Organometallics* **1998**, *17*, 3034–3043. (b) Long, N. J.; Martin, A. J.; Biani, F. F.; Zanello, P. *J. Chem. Soc., Dalton Trans.* **1998**, 2017–2021.

(20) Lavastre, O.; Plass, J.; Bachmann, P.; Guesmi, S.; Moinet, C.; Dixneuf, P. H. *Organometallics* **1997**, *16*, 184–189.

(21) (a) Narvor, N. L.; Lapinte, C. *Organometallics* **1995**, *14*, 634–639. (b) Weyland, T.; Lapinte, C.; Frapper, G.; Calhorda, M. J.; Halet, J.-F.; Toupet, L. *Organometallics* **1997**, *16*, 2024–2031. (c) Weyland, T.; Costuas, K.; Mari, A.; Halet, J.-F.; Lapinte, C. *Organometallics* **1998**, *17*, 5569–5579. (d) Weyland, T.; Costuas, K.; Toupet, L.; Halet, J.-F.; Lapinte, C. *Organometallics* **2000**, *19*, 4228–4239.

(22) Sato, M.; Sekino, M. *J. Organomet. Chem.* **1993**, *444*, 185–190.

(23) Kubas, G. J. *Inorg. Synth.* **1979**, *19*, 90–91.

tate. After stirring for half an hour, the precipitate was obtained by filtration. The yellow powder was redissolved in 5 mL of dichloromethane, and the solution was chromatographed on an alumina column. The product was collected as the first band using dichloromethane–petroleum ether (1:5) as an eluate. Yield: 54%. Anal. Calcd for $C_{88}H_{70}Fe_2P_4Ru_2 \cdot CH_2Cl_2$: C, 64.78; H, 4.40. Found: C, 64.54; H, 4.57. ES-MS: m/z (%) 1566 (100) $[M]^+$, 721 (66) $[Cp(dppf)Ru]^+$. IR (KBr, cm^{-1}): ν 2062m (C=C). 1H NMR ($CDCl_3$, ppm): δ 7.89–6.93 (m, 44H, C_6H_5 , C_6H_4), δ 5.30 (s, 2H, CH_2Cl_2), δ 5.40, 4.29, 4.18, 3.96 (four singlets, 16H, $(C_5H_4)_2Fe$) and 4.29 (s, 10H, CpRu). ^{31}P NMR (CD_2Cl_2): δ 55.4 (s). UV–vis (CH_2Cl_2): λ_{max}/nm ($\epsilon/M^{-1} cm^{-1}$) = 276 (26822), 365 (50980).

[[Cp(dppf)Ru] $_2$ (C=C–R–C=C)] (R = 1,4-naphthalenediyl, 3). The synthetic procedure to prepare this compound was the same as that of **1** except for the use of 1,4-bis-(trimethylsilylethynyl)naphthalene instead of 1,4-bis-(trimethylsilyl)-1,3-butadiyne. Yield: 50%. Anal. Calcd for $C_{92}H_{72}Fe_2P_4Ru_2$: C, 68.41; H, 4.49. Found: C, 68.69; H, 4.38. ES-MS: m/z (%) 1616 (100) $[M]^+$, 721 (12) $[Cp(dppf)Ru]^+$. IR (KBr, cm^{-1}): ν 2066m (C=C). 1H NMR ($CDCl_3$, ppm): δ 7.94–7.09 (m, 46H, C_6H_5 , $C_{10}H_6$), δ 5.40, 4.31, 4.11, 3.96 (four singlets, 16H, $(C_5H_4)_2Fe$), and 4.41 (s, 10H, CpRu). ^{31}P NMR (CD_2Cl_2): δ 55.8 (s). UV–vis (CH_2Cl_2): λ_{max}/nm ($\epsilon/M^{-1} cm^{-1}$) = 298 (33130), 429 (39050).

[[Cp(dppf)Ru] $_2$ (C=C–R–C=C)] (R = 1,10-anthracenediyl, 4). The synthetic preparation of this compound was the same as that of **1** except for the use of 9,10-bis(trimethylsilylethynyl)anthracene instead of 1,4-bis(trimethylsilyl)-1,3-butadiyne. Yield: 22%. Anal. Calcd for $C_{96}H_{74}Fe_2P_4Ru_2$: C, 69.24; H, 4.48. Found: C, 69.26; H, 4.87. ES-MS(m/z): 1666 (100) $[M]^+$, 722 (26) $[Cp(dppf)Ru]^+$. IR (KBr, cm^{-1}): ν 2045m (C=C). 1H NMR ($CDCl_3$, ppm): δ 8.03–7.10 (m, 48H, C_6H_5 , $C_{14}H_8$), δ 5.42, 4.76, 4.27, 3.95 (four singlets, 16H, $(C_5H_4)_2Fe$) and 4.27 (s, 10H, CpRu). ^{31}P NMR (CD_2Cl_2): δ 55.2 (s). UV–vis (CH_2Cl_2): λ_{max}/nm ($\epsilon/M^{-1} cm^{-1}$) = 295 (52100), 537 (31950).

[[Cp(dppf)Ru] $_2$ {Cu(MeCN) $_2$ (C=C–C=C)}](ClO $_4$) $_2$ (5-(ClO $_4$) $_2$). To a dichloromethane (15 mL) solution of **1** (50.0 mg, 0.033 mmol) was added a dichloromethane (5 mL) solution of $[Cu(MeCN)_4](ClO_4)$ (22.0 mg, 0.066 mmol). After the solution was stirred at room temperature for 12 h, the color changed from orange to olive. The solution was then obtained by filtration, and the filtrate was layered with petroleum ether to afford olive crystals. Yield: 57%. Anal. Calcd for $C_{86}H_{72}Cl_2Cu_2Fe_2N_2P_4Ru_2O_8$: C, 54.44; H, 3.83; N, 1.48. Found: C, 54.01; H, 3.75; N, 1.42. ES-MS: m/z (%) 1490 (96) $\{[Cp(dppf)Ru]_2(C=C–C=C)\}^+$, 807 (5) $\{[Cp(dppf)Ru]_2Cu_2(C=C–C=C)\}^{2+}$, 721 (100) $[Cp(dppf)Ru]^+$. IR (KBr, cm^{-1}): ν 1860m (C=C), 1089s (ClO_4). 1H NMR (CD_3CN , ppm): δ 7.83–6.62 (m, 40H, C_6H_5), δ 4.78, 4.65, 4.56, 4.43 (four singlets, 16H, $(C_5H_4)_2Fe$), δ 4.99 (s, 10H, CpRu), and δ 1.95 (s, 6H, CH_3CN). ^{31}P NMR (CD_2Cl_2): δ 51.5 (s). UV–vis (CH_2Cl_2): λ_{max}/nm ($\epsilon/M^{-1} cm^{-1}$) = 280 (48330), 374 (10730).

[[Cp(dppf)Ru] $_2$ (C=C–C=C)](PF $_6$) (1a(PF $_6$)). To a dichloromethane (20 mL) solution of **1** (50.0 mg, 0.034 mmol) was added ferrocenium hexafluorophosphate (11.3 mg, 0.034 mmol). The solution was stirred at room temperature for half an hour with the color changing from orange to green. After the solution was concentrated to 3 mL by evaporating the solvent, diethyl ether was added to produce a precipitate. After filtering, the precipitate was washed with 10 mL of diethyl ether three times. Yield: 94%. Anal. Calcd for $C_{82}H_{66}F_6Fe_2P_5Ru_2 \cdot CH_2Cl_2$: C, 57.99; H, 3.99. Found: C, 57.41; H, 3.83. ES-MS: m/z (%) 1637 (1) $[M]^+$, 1490 (38) $[M - (PF_6)]^+$, 749 (41) $[M - (PF_6)]^{2+}$, 721 (100) $[Cp(dppf)Ru]^+$. IR (KBr, cm^{-1}): 1966 m, 1855 s (C=C), 840 s (PF $_6$). ^{31}P NMR (CD_2Cl_2): δ 52.0 (s), –144.6 (septet, PF $_6$). UV–vis (CH_2Cl_2): λ_{max}/nm ($\epsilon/M^{-1} cm^{-1}$) = 359 (7990), 421 (3760).

[[Cp(dppf)Ru] $_2$ (C=C–R–C=C)](PF $_6$) (R = 1,4-naphthalenediyl, 3a(PF $_6$)). The synthetic preparation of this compound was the same as that of **1a(PF $_6$)** using **3** instead of

Table 1. Crystallographic Data for 1·3CH $_2$ Cl $_2$ and 5(ClO $_4$)(SbF $_6$)·CH $_2$ Cl $_2$

	1·3CH $_2$ Cl $_2$	5(ClO $_4$)(SbF $_6$)·CH $_2$ Cl $_2$
empirical formula	C $_{85}H_{72}Cl_6Fe_2P_4Ru_2$	C $_{87}H_{74}Cl_3Cu_2F_6Fe_2N_2O_4P_4Ru_2Sb$
temp, K	293(2)	293(2)
space group	$P2_1$	$P2_1$
<i>a</i> , Å	11.4543(3)	14.0106(3)
<i>b</i> , Å	24.8203(6)	12.4532(3)
<i>c</i> , Å	14.0568(2)	24.152
β , deg	109.0530(10)	94.7640(10)
<i>V</i> , Å 3	3777.40(14)	4199.42(14)
<i>Z</i>	2	2
ρ_{calcd} , g/cm $^{-3}$	1.533	1.675
μ , mm $^{-1}$	1.111	1.735
radiation (λ , Å)	0.71073	0.71073
R1(F_o) a	0.0684	0.0737
wR2(F_o) b	0.1505	0.1663
GOF	1.211	1.199

$$^a R1 = \sum |F_o - F_c| / \sum F_o. \quad ^b wR2 = \sum [w(F_o^2 - F_c^2)] / \sum [w(F_o^2)]^{1/2}.$$

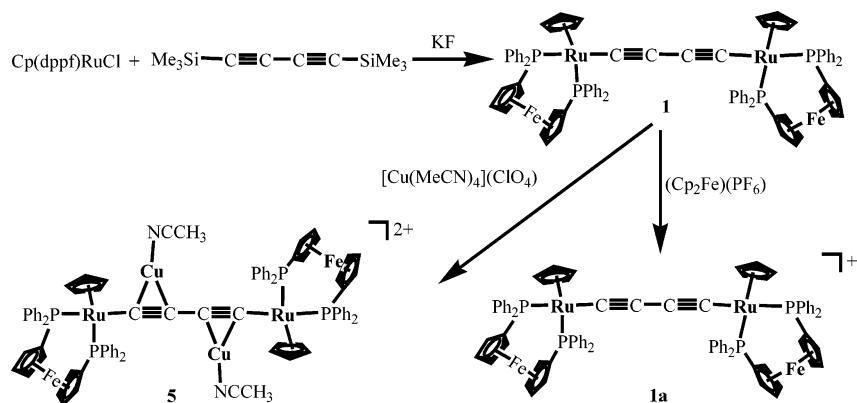
1 to give a blue product. Yield: 90%. Anal. Calcd for $C_{92}H_{72}F_6Fe_2P_5Ru_2$: C, 62.77; H, 4.12. Found: C, 62.44; H, 3.98. ES-MS: m/z (%) 1760 (2) $[M]^+$, 1616 (10) $[M - PF_6]^+$, 722 (100) $[Cp(dppf)Ru]^+$. IR (KBr, cm^{-1}): ν 1974 m (C=C), 840 s (PF $_6$). ^{31}P NMR (CD_2Cl_2): δ 51.74 (s), –144.3 (septet, PF $_6$). UV–vis (CH_2Cl_2): λ_{max}/nm ($\epsilon/M^{-1} cm^{-1}$) = 240 (77280), 375 (10150), 650 (17950).

[[Cp(dppf)Ru] $_2$ (C=C–R–C=C)](PF $_6$) (R = 1,10-anthracenediyl, 4a(PF $_6$)). The synthetic preparation of this compound was the same as that of **1a(PF $_6$)** using **4** instead of **1** to give a blue product. Yield: 87%. Anal. Calcd for $C_{96}H_{74}F_6Fe_2P_5Ru_2$: C, 63.69; H, 4.12. Found: C, 63.05; H, 4.01. ES-MS (m/z): 1811 (3) $[M]^+$, 1666 (100) $[M - (PF_6)]^+$. IR (KBr, cm^{-1}): 1946 m (C=C), 840 s (PF $_6$). ^{31}P NMR (CD_2Cl_2): δ 52.16 (s), –143.9 (septet, PF $_6$). UV–vis (CH_2Cl_2): λ_{max}/nm ($\epsilon/M^{-1} cm^{-1}$) = 252 (86800), 404 (12180), 790 (36940), 880 (25860).

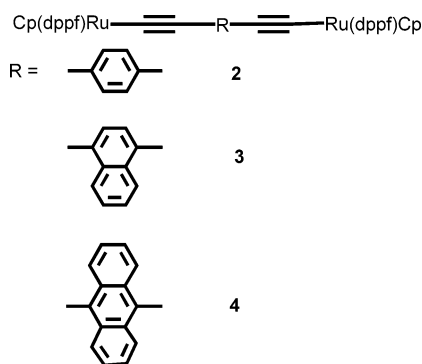
Crystal Structural Determination. Crystals of 1·3CH $_2$ Cl $_2$ and 5(ClO $_4$)(SbF $_6$)·CH $_2$ Cl $_2$ (prepared by metathesis of perchlorate in 5(ClO $_4$) $_2$ with sodium hexafluoroantimonate) suitable for X-ray crystallography were grown by layering petroleum ether onto the dichloromethane solutions. Single crystals sealed in capillaries with mother liquors were measured on a SIEMENS SMART CCD diffractometer by ω scan technique at room temperature using graphite-monochromated Mo K α (λ = 0.71073 Å) radiation. An absorption correction by SADABS was applied to the intensity data. The structures were solved by direct methods, and the heavy atoms were located from the E-map. The remaining non-hydrogen atoms were determined from the successive difference Fourier syntheses. All non-hydrogen atoms were refined anisotropically except those mentioned otherwise. The hydrogen atoms were generated geometrically and refined with isotropic thermal parameters. The structures were refined on F^2 by full-matrix least-squares methods using the SHELXL-97 program package. 24 The crystallographic data of 1·3CH $_2$ Cl $_2$ and 5(ClO $_4$)(SbF $_6$)·CH $_2$ Cl $_2$ are summarized in Table 1.

Physical Measurements. Elemental analyses (C, H, N) were performed on a Perkin-Elmer Model 240C automatic instrument. The electrospray mass spectra (ES-MS) were recorded on a Finnigan LCQ mass spectrometer using dichloromethane–methanol as mobile phase. The UV–vis–NIR spectra were measured on a Perkin-Elmer Lambda 900 UV–vis–NIR spectrometer. The IR spectra were recorded on a Magna 750 FT-IR spectrophotometer using KBr pellets. The ^{31}P NMR spectra (202.3 MHz) were performed on a Varian UNITY-500 spectrometer with 85% H $_3$ PO $_4$ as an external standard. The cyclic voltammogram (CV) and differential pulse

(24) Sheldrick, G. M. *SHELXL-97, Program for the Refinement of Crystal Structures*; University of Göttingen: Göttingen, Germany, 1997.

Scheme 1. Synthetic Route to C₄-Containing Compounds

Scheme 2



voltammogram (DPV) were made with a potentiostat/galvanostat Model 263A in dichloromethane solutions containing 0.1 M (Bu₄N)(PF₆) as supporting electrolyte. CV was performed at a scan rate of 100 mV s⁻¹. DPV was measured at a rate of 20 mV s⁻¹ with a pulse height of 40 mV. Platinum and glassy graphite were used as counter and working electrodes, respectively, and the potential was measured against a Ag/AgCl reference electrode. The potential measured was always referenced to the half-wave potentials of the ferrocenium/ferrocene couple ($E_{1/2} = 0$).

Results and Discussion

Syntheses and Characterization. Heterotetranuclear Ru^{II}Fe^{II} diyndiyl compounds **1** (Scheme 1) and **3** and **4** (Scheme 2) were readily prepared via fluoride-catalyzed^{14b} desilylation of Me₃Si-C≡C-R-C≡C-SiMe₃ (R = 0; 1,4-naphthalenediyl; 9,10-anthracenediyl) in the presence of Cp(dppf)RuCl. Compound **2** was isolated as a yellow precipitate by reaction of 2 equiv of Cp(dppf)RuCl with 1,4-diethynylbenzene in the presence of potassium hexafluorophosphate and then by addition of 3 equiv of sodium methoxide.^{20,21a} No attempt was made to isolate the possibly intermediate bis(vinylidene) complex in the reaction.^{21a} As shown in Scheme 1, treatment of **1** with 2 equiv of [Cu(MeCN)₄](ClO₄) afforded Ru^{II}Fe^{II}Cu^I₂ heterohexanuclear compound **5**(ClO₄)₂ through π -bonding of the acetylides to Cu^I centers. The Ru^{II}Fe^{II} mixed-valence compounds **1a**(PF₆), **3a**(PF₆), and **4a**(PF₆) were accessible by controlled oxidation of **1**, **3**, and **4** with equimolar ferrocenium hexafluorophosphate, respectively. Attempts to isolate the one-electron-oxidized product of **2** failed because of extreme instability of this mixed-valence species. The Ru^{II}Fe^{II} mixed-valence compound **1a** could be further oxidized by silver hexafluorophosphate at -78 °C to

produce a dark blue Ru^{III}Fe^{III} compound, but it is highly unstable and could not be isolated at room temperature.

Elemental analyses (C, H, N) coincide well with the calculated values for all of the compounds. Positive ion ES-MS of the neutral compounds **1–4** show molecular ion fragment [M]⁺ as the principal peak. Both [M]⁺ and [M - (PF₆)]⁺ fragment peaks occur in the ES-MS of **1a**(PF₆), **3a**(PF₆), and **4a**(PF₆) with Ru^{II}Fe^{II} mixed-valence. For the Ru^{II}Fe^{II}Cu^I₂ compound **5**(ClO₄)₂, the peaks for fragments [Cp(dppf)Ru]₂(C≡C-C≡C)⁺ and [Cp(dppf)Ru]₂Cu₂(C≡C-C≡C)²⁺ are observed.

The IR spectra of compounds **1–4** display vibrational frequencies of moderate intensity in the range 1968–2066 cm⁻¹ due to typical C≡C triple bonding. In the IR spectra of Ru^{II}Fe^{II} mixed-valence products **1a**(PF₆), **3a**(PF₆), and **4a**(PF₆), the ν (C≡C) shows an obvious shift (100–120 cm⁻¹) to lower wavenumber relative to that of the Ru^{II}₂ parent compounds. As demonstrated in other diacetylide-linked ruthenium complexes,^{14,15} the C≡C bonding intensity is reduced with oxidation of Ru^{II} into Ru^{III} centers, indicating a diminution of the bond order and an increasing contribution of the cumulenic resonance structure.^{14a,15} In the IR spectrum of heterohexanuclear compound **5**(ClO₄)₂, the ν (C≡C) occurs at 1860 cm⁻¹, revealing a significant red shift (ca. 108 cm⁻¹) relative to that observed in **1**. Accordingly, $\eta^2(\pi)$ -bonding of C≡C-C≡C to two Cu^I atoms weakens remarkably the C≡C bonding.

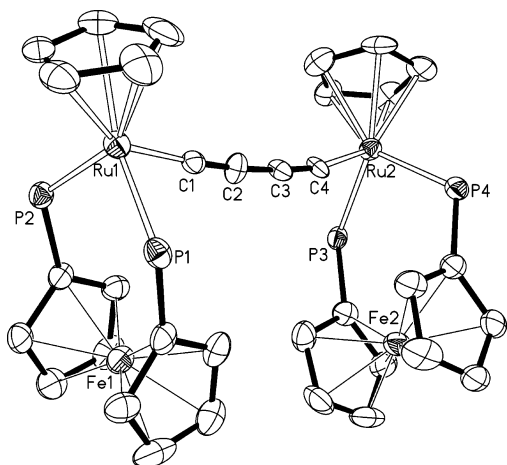
In the ³¹P NMR spectra of **1–4**, only a singlet at ca. 55.0 ppm is observed. This signal is shifted to around 52.0 ppm in the mixed-valence compounds **1a**(PF₆), **3a**(PF₆), and **4a**(PF₆). The phosphorus multiplets of hexafluorophosphate appear at ca. -144.0 ppm. The ³¹P NMR spectrum of Ru^{II}Fe^{II}Cu^I₂ heterohexanuclear compound **5** shows a singlet at 51.5 ppm, revealing a slight shift to high field compared with that in its precursor compound **1**.

Crystal Structures. Compounds **1** and **5**(ClO₄)(SbF₆) were characterized by X-ray crystallography. Selected atomic distances and bond angles are listed in Table 2. Perspective views of **1** and the complex cation of **2** are depicted in Figures 1 and 2, respectively.

Compound **1** consists of two Cp(dppf)Ru units bridged by C≡C-C≡C through σ -coordination. The Cp and dppf are oriented in the same side to adopt a cisoid conformation, as shown in Figure 1. The quasi-linearity of the Ru-C≡C-C≡C-Ru array is reflected in the quasi-linear Ru-C≡C [170.8(10)° and 176.6(11)°] and C≡C-C angles [174.5(13)° and 175.4(13)°]. The RuLRu separa-

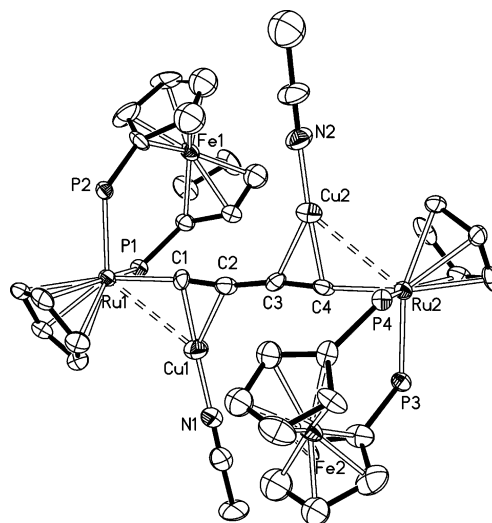
Table 2. Selected Bond Distances (Å) and Angles (deg) for **1** and **5(ClO₄)(SbF₆)**

	1	5(ClO₄)(SbF₆)	1	5(ClO₄)(SbF₆)	
Ru1–C1	2.029(12)	2.012(16)	Ru2–C4	1.974(11)	2.000(16)
Ru1–C11	2.206(13)	2.245(19)	Ru2–C21	2.235(13)	2.241(19)
Ru1–C12	2.238(15)	2.246(17)	Ru2–C22	2.229(14)	2.234(17)
Ru1–C13	2.226(15)	2.252(19)	Ru2–C23	2.226(14)	2.23(2)
Ru1–C14	2.230(14)	2.276(18)	Ru2–C24	2.216(13)	2.232(17)
Ru1–C15	2.263(13)	2.239(19)	Ru2–C25	2.248(12)	2.264(16)
Ru1–P1	2.254(3)	2.322(5)	Ru2–P3	2.264(3)	2.308(5)
Ru1–P2	2.259(3)	2.308(5)	Ru2–P4	2.270(3)	2.309(5)
C1–C2	1.181(15)	1.23(2)	C2–C3	1.410(17)	1.38(2)
Ru–Cu1		2.936(3)	Ru2–Cu2		2.964(3)
Cu1–N1		1.869(19)	Cu2–N2		1.824(19)
Cu1–C1		1.950(18)	Cu2–C3		2.105(18)
Cu1–C2		2.133(18)	Cu2–C4		1.940(19)
C1–Ru1–P1	87.2(3)	88.9(5)	C4–Ru2–P3	88.6(3)	88.0(5)
C1–Ru1–P2	85.7(3)	87.4(5)	C4–Ru2–P4	87.4(4)	90.1(6)
P1–Ru1–P2	97.76(12)	98.36(18)	P3–Ru2–P4	97.53(12)	97.38(18)
C2–C1–Ru1	176.6(11)	171.8(16)	C3–C4–Ru2	170.8(10)	174.7(14)
C1–C2–C3	174.5(13)	167.5(17)	C4–C3–C2	175.4(13)	168.0(18)
N1–Cu1–C1		171.0(8)	N2–Cu2–C4		174.2(9)
N1–Cu1–C2		139.3(7)	N2–Cu2–C3		144.9(7)
C1–Cu1–C2		34.8(6)	C4–Cu2–C3		35.9(6)

**Figure 1.** ORTEP drawing of **1** with atom-labeling scheme showing 30% thermal ellipsoids. Phenyl rings on the phosphorus atoms are omitted for clarity.

tion is 7.741 Å through bridging C≡C–C≡C, which is comparable with those observed in other C₄-bridged dinuclear Ru^{II} compounds.^{14,15} The Ru–C and Ru–P distances are in the normal ranges and in accordance with those found in compounds [$\{\text{Cp}(\text{PPh}_3)_2\text{Ru}\}_2(\text{C}\equiv\text{C}-\text{C}\equiv\text{C})$]¹⁴ and [$\{\text{Cp}^*(\text{dppf})\text{Ru}\}_2(\text{C}\equiv\text{C}-\text{C}\equiv\text{C})$].¹⁵ The C=C lengths [1.181(15) and 1.220(16) Å] are typical of carbon–carbon triple bonding.

In contrast with the cisoid conformation in **1**, the complex cation [$\{\text{Cp}(\text{dppf})\text{Ru}\}_2\{\text{Cu}(\text{MeCN})_2\}_2(\text{C}\equiv\text{C}-\text{C}\equiv\text{C})$]²⁺ of compound **5(ClO₄)(SbF₆)** exhibits a transoid conformation with Cp and dppf oriented in opposite sides (Figure 2). Two Cu(MeCN) fragments, bonded to C≡C–C≡C through $\eta^2(\pi)$ -coordination, are also arranged in a trans orientation. Compared with those in **1**, the Ru–P, Ru–Cp, and Ru_LRu distances become slightly longer in compound **5(ClO₄)(SbF₆)**. Furthermore, $\eta^2(\pi)$ -coordination of the acetylide to Cu^I atoms results in the C=C and C–C distances of the C₄ ligand appreciably elongated (0.049 Å) and shortened (0.03 Å), respectively.²⁵ The Ru–Cu distances are 2.936(3) and 2.964(3)

**Figure 2.** ORTEP drawing of the complex cation of **5(ClO₄)(SbF₆)** with atom-labeling scheme showing 30% thermal ellipsoids. Phenyl rings on the phosphorus atoms are omitted for clarity.

Å, indicating that a weak Ru–Cu contact is operative. The Ru1...Ru2 separation is 7.852 Å, a little elongated relative to that in **1**. The Cu1 atom is coordinated to acetonitrile and C≡C through π -coordination.

Redox Properties. The redox chemistry of compounds **1–5(ClO₄)₂** was investigated by cyclic and pulse differential voltammetry in 0.1 M dichloromethane solution of (Bu₄N)(PF₆). The electrochemical data are presented in Table 3, and a plot of the cyclic voltammogram (CV) and pulse differential voltammogram (DPV) of compound **1** is depicted in Figure 3.

The free ligand of dppf exhibits a reversible oxidation wave at $E_{1/2} = +0.190$ V (referenced to ferrocene) in dichloromethane solutions containing 0.1 M (Bu₄N)(PF₆) as supporting electrolyte. This reversible oxidation process shows a positive shift to +0.490 V in the compound Cp(dppf)RuCl, in which oxidation of Ru^{II} into Ru^{III} occurs at +0.077 V.²⁶ From the electrochemical

(25) Mihan, S.; Sünkel, K.; Beck, W. *Chem. Eur. J.* **1999**, *5*, 745–753.(26) Wu, I.-Y.; Lin, J. T.; Luo, J.; Sun, S.-S.; Li, C.-S.; Lin, K. J.; Tsai, C.; Hsu, C.-C.; Lin, J.-L. *Organometallics* **1997**, *16*, 2038–2048.

Table 3. Electrochemical Data for Compounds 1–4^a

compound	$E_{1/2}$ (A)	$E_{1/2}$ (B)	$E_{1/2}$ (C) ^b	$E_{1/2}$ (D) ^c	$E_{1/2}$ (E) ^b	$\Delta E_{1/2}$ ^d	K_c ^e
Cp(dppf)RuCl		0.077 ^f		0.490 ^f			
1	-0.680	-0.030	+0.371	+0.520	+0.820	+0.650	9.7×10^{11}
2	-0.270	-0.006	+0.430	+0.560	+0.830	+0.264	2.9×10^4
3	-0.357	-0.086	+0.448	+0.550	+0.860	+0.271	3.8×10^4
4	-0.477	-0.187	+0.510	+0.510	+0.828	+0.290	8.0×10^4

^a Potential data in volts vs Fc^+/Fc are from single scan cyclic voltammograms recorded at 25 °C. Detailed experimental conditions are given in the Experimental Section. ^b Redox processes $E_{1/2}$ (C) and $E_{1/2}$ (E) are quasi-reversible or irreversible and may be from oxidation of the ruthenium centers. ^c Irreversible process $E_{1/2}$ (D) is from oxidation of ferrocenyl in dppf ligand. ^d $\Delta E_{1/2} = E_{1/2}$ (B) - $E_{1/2}$ (A) denotes the potential difference between redox processes A and B. ^e The comproportionation constants, K_c , were calculated by the formula $K_c = \exp(\Delta E_{1/2}/25.69)$ at 298 K.³³ ^f The $E_{1/2}$ at 0.077 and 0.490 V correspond to oxidation of the Ru^{II} center and ferrocenyl of Cp(dppf)RuCl, respectively.

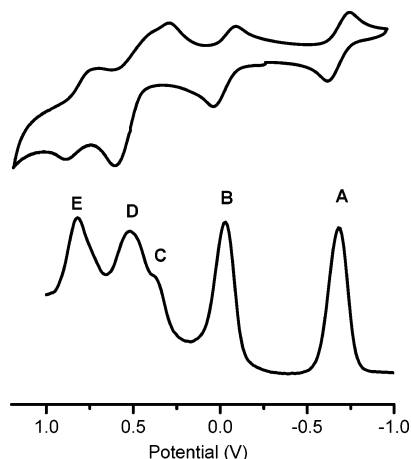


Figure 3. Cyclic and differential pulse voltammograms (CV and DPV) of compound **1** in 0.1 M dichloromethane solution of $(\text{Bu}_4\text{N})(\text{PF}_6)$. The scan rate is 100 mV s^{-1} for CV and 20 mV s^{-1} for DPV.

data presented in Table 3, it is revealed that in $\text{Ru}^{\text{II}}_2\text{-Fe}^{\text{II}}_2$ heterotetranuclear diyndiyl complexes **1–4** the redox potentials of ferrocenyl and Ru^{II} centers show slightly positive and negative shifts, respectively, relative to those in the precursor compound Cp(dppf)RuCl.

As depicted in Figure 3, five redox waves are observed in the CV and DPV of compound **1**. While waves A and B are reversible, waves C, D, and E are quasi-reversible or irreversible. Waves A and B are ascribable to step-wise one-electron oxidation of $\text{Ru}_2^{\text{II,II}}$ into $\text{Ru}_2^{\text{II,III}}$ and $\text{Ru}_2^{\text{III,III}}$ species, corresponding to the redox couples $\text{Ru}_2^{\text{II,II}}/\text{Ru}_2^{\text{II,III}}$ and $\text{Ru}_2^{\text{II,III}}/\text{Ru}_2^{\text{III,III}}$, respectively. The large potential separation ($\Delta E_{1/2} = 0.650$ V) between the two one-electron processes reflects a remarkable electronic delocalization along the molecular rod. The comproportionation constant K_c is 9.74×10^{10} , which is comparable to those found in compounds [$\{\text{Cp}(\text{PPh}_3)_2\text{Ru}\}_2(\text{C}\equiv\text{C}-\text{C}\equiv\text{C})$] (1.7×10^{11})^{14a} and [$\{\text{Cp}^*(\text{dppe})\text{Ru}\}_2(\text{C}\equiv\text{C}-\text{C}\equiv\text{C})$] (9.70×10^{11}).¹⁵ By reference to dinuclear diyndiyl rhenium compounds containing redox termini Cp(PPh_3)₂Ru¹⁴ and Cp*(dppe)Ru,¹⁵ waves C and E may also originate from oxidation of the ruthenium centers, although the two redox processes are not reversible. Since wave D is comparatively broad and its potential is close to that of the Fe^{II} center in the parent compound Cp(dppf)RuCl, it is tentatively assigned to oxidation of Fe^{II} centers in compound **1**. As the two closely spaced one-electron processes are irresolvable by CV and DPV, it appears that the two ferrocenyls in **1** are oxidized simultaneously.

In contrast to the reversible redox behavior of compound **1**, the cyclic voltammogram of $\text{Ru}^{\text{II}}_2\text{Fe}^{\text{II}}_2\text{Cu}^{\text{I}}_2$

heterohexanuclear compound **5**(ClO₄)₂ displays only two irreversible oxidation processes at +0.24 and +0.52 V and one reduction peak at +0.19 V. Obviously, the redox reversibility is damaged by $\eta^2(\pi)$ -bonding of the acetylides to two Cu^{I} atoms. Consequently, irreversible redox behavior of compound **5**(ClO₄)₂ excludes evaluating unambiguously whether the π -bonded Cu^{I} could act to enhance or reduce electronic interaction between two redox termini Cp(dppf)Ru relative to that found in the parent compound **1**.

Although waves C, D, and E are irreversible in compounds **2–4**, their redox behavior is similar to that of **1**. The potential difference $\Delta E_{1/2}$ between reversible waves A and B due to the electronic delocalization of mixed-valence species $\text{Ru}_2^{\text{II,III}}$ is in the range 0.264–0.290 V. It is noteworthy that the $\Delta E_{1/2}$ and K_c (Table 3) of compounds **2–4** increase in the order **2** < **3** < **4**, which agrees well with the increasing order of the conjugating range in the bridging ligands. Thus, the degree of electronic delocalization in mixed-valence species [$\{\text{Cp}(\text{dppf})\text{Ru}\}_2(\text{C}\equiv\text{C}-\text{R}-\text{C}\equiv\text{C})$]⁺ is finely tunable by changing the conjugating range of the R substituent.¹⁹

UV–Vis–NIR Spectra. Besides the intense ligand-centered absorption bands at 200–310 nm, a band at ca. 350–550 nm occurs in the UV–vis spectra of compounds **1–4**, ascribed to a Ru^{II} –ligand MLCT transition. This band becomes weaker in the one-electron-oxidized compounds. Furthermore, new bands at a lower wavelength (420–880 nm) appear, assigned tentatively to ligand→ Ru^{III} LMCT transitions, which is a consequence of the oxidation of one Ru^{II} into Ru^{III} .

The most characteristic band in the mixed-valence $\text{Ru}_2^{\text{II,III}}$ compounds **1a**(PF₆), **3a**(PF₆), and **4a**(PF₆) is the strong absorption in the near-IR due to intervalence charge transfer (IVCT) transition between Ru^{II} and Ru^{III} centers (Table 4), which are absent in the spectra of the neutral $\text{Ru}_2^{\text{II,II}}$ complexes **1**, **3**, and **4**. Figure 4 shows the IVCT band of **1a**(PF₆) measured in dichloromethane at 298 K. As listed in Table 4, this band is observed at 906 nm for **1a**(PF₆) with the extinction coefficient (ϵ) being 16 400 $\text{M}^{-1} \text{cm}^{-1}$. Solvent independence of the λ_{max} over a wide range of solvent polarity is a clear indication of the average solvation of a delocalized $\text{Ru}_2^{\text{II,III}}$ system. The observed half-width $\Delta\nu_{1/2}$ (3666 cm^{-1}) is markedly narrower than the widths (5040 cm^{-1}) predicted from the relationship in the equation $\Delta\nu_{1/2} = (2310\nu_{\text{max}})^{1/2}$, established by Hush for the class II mixed-valence system.^{11b,21d,27–29} It has been demonstrated that a large comproportionation constant ($K_c = 9.74 \times 10^{10}$ for **1a**(PF₆)), high extinction coefficient ($\epsilon = 16 400 \text{ M}^{-1} \text{cm}^{-1}$) of the IVCT band, solvent independence of λ_{max} , and narrow half-width ($\Delta\nu_{1/2}$) are characteristics of class

Table 4. Visible–Near-Infrared Spectral Data for Ru₂^{II,III} Mixed-Valence Compounds 1a(PF₆), 3a(PF₆), and 4a(PF₆) in Dichloromethane at 298 K

compound	λ_{\max} (nm)	ϵ_{\max} (cm ⁻¹ M ⁻¹)	ν_{\max} (cm ⁻¹)	$\Delta\nu_{\text{obsd}}$ (cm ⁻¹) ^a	$\Delta\nu_{\text{calcd}}$ (cm ⁻¹) ^b	V_{ab}' (eV) ^c	V_{ab} (eV) ^d
1a(PF ₆)	906	16 400	11 037	3666	5040	0.27	0.68
3a(PF ₆)	1312	15 950	7622	2786	4191	0.12	0.47
4a(PF ₆)	1110	19 110	9009	2753	4557	0.14	0.56

^a $\Delta\nu_{\text{obsd}}$ is the observed half-width of the IVCT band. ^b $\Delta\nu_{\text{calcd}}$ is the calculated half-width from the equation $\Delta\nu_{1/2} = (2310\nu_{\max})^{1/2}$ by Hush's theoretical analysis. ^c $V_{\text{ab}}' = \{[2.05 \times 10^{-2}(\nu_{\max}\epsilon_{\max}\Delta\nu_{1/2})^{1/2}]/R\}$ from Hush's theoretical analysis for a weakly coupling system of class II mixed-valence compounds, where ϵ_{\max} , ν_{\max} , and $\Delta\nu_{1/2}$ are the molar extinction coefficient, the absorption maximum in wavenumbers, and the bandwidth at half-maximum height in wavenumbers, respectively; the metal–metal distance R is 7.741 Å in 1a(PF₆) and 12.242 Å in 3a(PF₆) and 4a(PF₆). ^d $V_{\text{ab}} = \nu_{\max}/2$ for delocalized class III mixed-valence compounds.

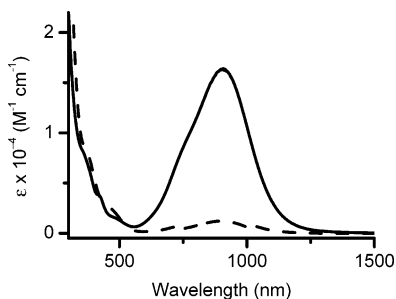


Figure 4. Visible–near-infrared spectra of **1** (dashed line) and **1a**(PF₆) (solid line) in dichloromethane, showing IVCT band of the mixed-valence compound **1a**(PF₆).

III mixed-valence compounds with electronic delocalization.^{27–29} Thus, **1a**(PF₆) is a typical class III mixed-valence compound according to Robin and Day classification.²⁹ The odd electron is delocalized over the Ru^{II}–C₄–Ru^{III} array, and the coupling parameter V_{ab} is simply related to the energy of the NIR band with $V_{\text{ab}} = \nu_{\max}/2$.^{11b,14a,15} The large V_{ab} (0.68 eV) of **1a**(PF₆) is characteristic of a class III mixed-valence system.^{11b,14a,15}

In the visible–near-infrared spectra of mixed-valence compounds **3a**(PF₆) and **4a**(PF₆) with a longer C≡C–R–C≡C bridge (R = 1,4-naphthalenediyl or 1,10-anthracenediyl), the IVCT bands occur at 1312 and 1110 nm with $\epsilon = 15\,950$ and $19\,110$ M⁻¹ cm⁻¹, respectively, in dichloromethane. Measurements of the IVCT band in different organic solvents such as chloroform, acetone, and acetonitrile show only slight shifts. The measured half-widths ($\Delta\nu_{1/2}$) are 2786 and 2753 cm⁻¹ for **3a**(PF₆) and **4a**(PF₆), respectively, which are significantly narrower compared with the calculated values (4191 cm⁻¹ for **3a**(PF₆) and 4557 cm⁻¹ for **4a**(PF₆)) by Hush's theoretical analysis for class II mixed-valence compounds. Therefore, the IVCT properties including their high intensity and small solvent effect, together with narrow half-widths, reveal that **3a**(PF₆) and **4a**(PF₆) are not typical Robin–Day class II mixed-valence compounds. Nevertheless, compared with the much higher value for class III mixed-valence compound **1a**(PF₆) ($K_c = 9.7 \times 10^{10}$), the relative low K_c values for **3a**(PF₆) (K_c

$= 3.8 \times 10^4$) and **4a**(PF₆) ($K_c = 3.8 \times 10^4$) are an indication of a weaker coupling between two ruthenium centers across a longer C≡C–R–C≡C bridge. As anticipated, the mixed-valence compounds **3a**(PF₆) and **4a**(PF₆) may be between electronic localization and delocalization.^{21a,29–33}

Conclusions

Designed syntheses of Ru^{II}₂Fe^{II}₂ heterotetranuclear diyndiyl compounds [$\{\text{Cp}(\text{dppf})\text{Ru}\}_2(\text{C}\equiv\text{C}-\text{R}-\text{C}\equiv\text{C})$] (R = 0, 1,4-benzenediyl; 1,4-naphthalenediyl; 1,10-anthracenediyl) and their one-electron-oxidized complexes [$\{\text{Cp}(\text{dppf})\text{Ru}\}_2(\text{C}\equiv\text{C}-\text{R}-\text{C}\equiv\text{C})$](PF₆) with mixed-valence were achieved. Reaction of [Cu(MeCN)₄](ClO₄) with **1** afforded Ru^{II}₂Fe^{II}₂Cu^I₂ heterohexanuclear compounds **5**(ClO₄)₂. While a remarkable electronic coupling is operative between two ruthenium centers across a bridging diacetylide, redox interaction between two ferrocenyl groups (iron centers) is undetectable by CV and DPV in compounds [$\{\text{Cp}(\text{dppf})\text{Ru}\}_2(\text{C}\equiv\text{C}-\text{R}-\text{C}\equiv\text{C})$]. Redox reversibility in **5**(ClO₄)₂ is damaged by π -bonding of the acetylides to Cu^I centers. The Ru₂^{II,III} compound **1a**(PF₆) belongs to a class III mixed-valence system with high electronic delocalization. From the IVCT behavior of **3a**(PF₆) and **4a**(PF₆) together with their redox properties, it appears that they are between electronic localization and delocalization.

Acknowledgment. This work was supported by NSFC (20171044, 20273074, 20490210, and 90401005), NSF of Fujian Province (E0420002 and E0310029), and the fund from the Chinese Academy of Sciences.

Supporting Information Available: Electrochemical plots of compounds **2–4** and visible–near-infrared spectra of mixed-valence compounds **3a**(PF₆) and **4a**(PF₆). X-ray crystallographic files in CIF format for the structure determination of compounds **1**·3CH₂Cl₂ and **5**(ClO₄)(SbF₆)·CH₂Cl₂. This material is available free of charge via the Internet at <http://pubs.acs.org>.

OM049086L

(27) Hush, N. S. *Prog. Inorg. Chem.* **1967**, *8*, 391.

(28) Richardson, D. E.; Taube, H. *Coord. Chem. Rev.* **1984**, *60*, 107–129.

(29) Robin, M. B.; Day, P. *Adv. Inorg. Chem. Radiochem.* **1967**, *10*, 247.

(30) Demadis, K. D.; Hartshorn, C. M.; Meyer, T. J. *Chem. Rev.* **2001**, *101*, 2655–2686.

(31) Brunshwig, B. S.; Creutz, C.; Sutin, N. *Chem. Soc. Rev.* **2002**, *31*, 168–184.

(32) Nelsen, S. F. *Chem. Eur. J.* **2000**, *6*, 581–588.

(33) Richardson, D. E.; Taube, H. *Inorg. Chem.* **1981**, *20*, 1278–1285.